Marquette University
e-Publications@Marquette

Biomedical Engineering Faculty Research and Publications

Biomedical Engineering, Department of

3-1-2014

Comparison of Adaptive Optics Scanning Light Ophthalmoscopic Fluorescein Angiography and Offset Pinhole Imaging

Toco Y.P. Chui
New York Eye and Ear Infirmary

Michael Dubow
New York Icahn School of Medicine at Mount Sinai

Alexander Pinhas
New York Icahn School of Medicine at Mount Sinai

Nishit Shah
New York Eye and Ear Infirmary

Alexander Gan
New York Eye & Ear Infirmary

See next page for additional authors

Accepted version. *Biomedical Optics Express*, Vol. 5, No. 4 (March 2014): 1173-1189. DOI. © 2014 Optical Society of America. Used with permission.

Authors
Toco Y.P. Chui, Michael Dubow, Alexander Pinhas, Nishit Shah, Alexander Gan, Rishard Weitz, Yusufu N. Sulai, Alfredo Dubra, and Richard B. Rosen

This article is available at e-Publications@Marquette: https://epublications.marquette.edu/bioengin_fac/322

***NOT THE PUBLISHED VERSION;* this is the author's final, peer-reviewed manuscript.** The published version may be accessed by following the link in the citation at the bottom of the page.

Comparison of adaptive optics scanning light ophthalmoscopic fluorescein angiography and offset pinhole imaging

Toco Y.P. Chui[1]
Department of Ophthalmology, New York Eye & Ear Infirmary
New York, NY
Michael Dubow[1,2]
Department of Ophthalmology, New York Eye & Ear Infirmary
Icahn School of Medicine at Mount Sinai
New York, NY
Alexander Pinhas[1,2]
Department of Ophthalmology, New York Eye & Ear Infirmary
Icahn School of Medicine at Mount Sinai
New York, NY
Nishit Shah[1]
Department of Ophthalmology, New York Eye & Ear Infirmary
New York, NY
Alexander Gan[1]
Department of Ophthalmology, New York Eye & Ear Infirmary
New York, NY

[Citation: Journal/Monograph Title, Vol. XX, No. X (yyyy): pg. XX-XX. DOI. This article is © [Publisher's Name] and permission has been granted for this version to appear in e-Publications@Marquette. [Publisher] does not grant permission for this article to be further copied/distributed or hosted elsewhere without the express permission from [Publisher].]

***NOT THE PUBLISHED VERSION;* this is the author's final, peer-reviewed manuscript.** The published version may be accessed by following the link in the citation at the bottom of the page.

Rishard Weitz[1]
Department of Ophthalmology, New York Eye & Ear Infirmary
New York, NY
Yusufu N. Sulai[3]
The Institute of Optics, University of Rochester
Rochester, NY
Alfredo Dubra[4,5,6]
Department of Biomedical Engineering, Marquette University
Department of Ophthalmology, Medical College of Wisconsin
Department of Biophysics, Medical College of Wisconsin
Milwaukee, WI
Richard B. Rosen[1,7,*]
Department of Ophthalmology, New York Eye & Ear Infirmary
Department of Ophthalmology, New York Medical College
Valhalla, NY

Abstract: Recent advances to the adaptive optics scanning light ophthalmoscope (AOSLO) have enabled finer *in vivo* assessment of the human retinal microvasculature. AOSLO confocal reflectance imaging has been coupled with oral fluorescein angiography (FA), enabling simultaneous acquisition of structural and perfusion images. AOSLO offset pinhole (OP) imaging combined with motion contrast post-processing techniques, are able to create a similar set of structural and perfusion images without the use of exogenous contrast agent. In this study, we evaluate the similarities and differences of the structural and perfusion images obtained by either method, in healthy control subjects and in patients with retinal vasculopathy including hypertensive retinopathy, diabetic retinopathy, and retinal vein occlusion. Our results show that AOSLO OP motion contrast provides perfusion maps comparable to those obtained with AOSLO FA, while AOSLO OP reflectance images provide additional information such as vessel wall fine structure not as readily visible in AOSLO confocal reflectance images. AOSLO OP offers a non-invasive alternative to AOSLO FA without the need for any exogenous contrast agent.

[Citation: Journal/Monograph Title, Vol. XX, No. X (yyyy): pg. XX-XX. DOI. This article is © [Publisher's Name] and permission has been granted for this version to appear in e-Publications@Marquette. [Publisher] does not grant permission for this article to be further copied/distributed or hosted elsewhere without the express permission from [Publisher].]

***NOT THE PUBLISHED VERSION;* this is the author's final, peer-reviewed manuscript.** The published version may be accessed by following the link in the citation at the bottom of the page.

1. Introduction

Intravenous (IV) fluorescein angiography (FA) is the clinical gold standard for assessing retinal vasculature, revealing the extent of disease and response to treatment [1]. Despite its utility, the IV injection of fluorescein dye is considered invasive, and has been reported to cause rare but potentially severe systemic adverse reactions [2–6]. Furthermore, with the limitations in axial and lateral resolution of standard fundus cameras, IV FA provides an incomplete visualization and differentiation of the inner and outer capillary plexuses, as described in human retinal histology [7]. Recent advances in adaptive optics imaging have been employed to overcome these limitations [8–17], and two major techniques are now being used to image the retinal microvasculature for the purposes of research and anticipated adaption into clinical practice [13, 14, 16, 18, 19]. Adaptive optics scanning light ophthalmoscope FA (AOSLO FA) is a confocal imaging technique that allows simultaneous acquisition of structural reflectance and functional perfusion images. The sensitivity of the technique permits the use of orally administered fluorescein which may have a safer side effect profile than conventional IV fluorescein [20, 21]. AOSLO offset pinhole (OP) imaging utilizes an off-center pinhole and has recently been described for the visualization of blood flow and microscopic features of the vascular wall [14, 16]. Coupled with motion contrast processing techniques [22–27], AOSLO OP imaging can reveal microvascular perfusion maps of the retinal vasculature, without the use of an exogenous contrast agent. In this study, we compare the information provided by AOSLO FA and AOSLO OP structural and perfusion maps, in imaging healthy and diseased retinal microvasculature.

2. **Methods**

2.1 Subjects

This study adhered to the tenets of the Declaration of Helsinki and was approved by the Institutional Review Board of the New York Eye and Ear Infirmary. Three healthy male subjects (3 eyes; age range 23-25 yo) and five patients (5 eyes), each with a single retinal pathology were recruited for this study. Inclusion criteria included

[Citation: Journal/Monograph Title, Vol. XX, No. X (yyyy): pg. XX-XX. DOI. This article is © [Publisher's Name] and permission has been granted for this version to appear in e-Publications@Marquette. [Publisher] does not grant permission for this article to be further copied/distributed or hosted elsewhere without the express permission from [Publisher].]

***NOT THE PUBLISHED VERSION;* this is the author's final, peer-reviewed manuscript.** The published version may be accessed by following the link in the citation at the bottom of the page.

normal anterior segment with clear phakic lens, pupil dilation of at least 5 mm, clear media and good central fixation with a best-corrected visual acuity (BCVA) better than 20/80. Eyes had minimal or no foveal edema evident by spectral domain optical coherence tomography (Heidelberg Spectralis HRA + OCT, Heidelberg Engineering Inc., Heidelberg, Germany). All three healthy subjects were self-reported healthy individuals with no significant past medical history and no clinical signs or symptoms of ocular pathology. The pathologies of the patients were: hypertensive retinopathy (HR; RR0095; 47 yo male), diabetic retinopathy (DR; RR0167; 49 yo female), macular drusen (RR0160; 37 yo female), central retinal vein occlusion (CRVO; RR0151; 62 yo female), and branch retinal vein occlusion (BRVO; RR0129; 55 yo female). Written informed consent was obtained after the nature and potential risks of the procedure were explained. All tested eyes were imaged with AOSLO FA and OP during the same visit, except for the BRVO patient, who was imaged with AOSLO OP 4 months after the initial AOSLO FA imaging session. BCVA was recorded for all subjects and patients before AOSLO imaging. Pupils were dilated with 1 drop of 2.5% phenylephrine hydrochloride ophthalmic solution (Bausch & Lomb Inc., Tampa, FL) and 1% tropicamide ophthalmic solution (Akorn Inc., Lake Forest, IL).

2.2 Preliminary ocular imaging

Prior to AOSLO imaging, color fundus photography (Topcon 3D OCT 2000, Topcon Corporation, Tokyo, Japan) was performed on all tested eyes. Conventional IV FA using either HRA-OCT (Heidelberg Spectralis, Heidelberg Engineering Inc., Heidelberg, Germany) or TRC 50IX Retinal Camera (Topcon Corporation, Tokyo, Japan) was performed on each of the five patients. No patient received both IV FA and AOSLO FA imaging on the same day. Regions of interest for AOSLO imaging were pre-identified on either the color fundus photographs or IV FAs. Axial length measurements of the tested eyes were obtained using an IOL Master (Carl Zeiss Meditec, Dublin, California). Individual retinal magnification factors were applied to the AOSLO images incorporating the measured axial lengths into the Emsley schematic eye model formula [28].

[Citation: Journal/Monograph Title, Vol. XX, No. X (yyyy): pg. XX-XX. DOI. This article is © [Publisher's Name] and permission has been granted for this version to appear in e-Publications@Marquette. [Publisher] does not grant permission for this article to be further copied/distributed or hosted elsewhere without the express permission from [Publisher].]

***NOT THE PUBLISHED VERSION;* this is the author's final, peer-reviewed manuscript.** The published version may be accessed by following the link in the citation at the bottom of the page.

2.3 AOSLO instrumentation

The AOSLO used in this experiment was a replica of the one described by Dubra and Sulai [29] with the visible channel modified for fluorescence imaging. In brief, three different light sources (488, 790 and 850 nm) which entered the eye as superimposed (coaxial), near-collimated 7.75 mm diameter beams were used for FA excitation, reflectance imaging and wavefront sensing respectively. All three beams localized onto a single spot on the fundus, which was rapidly scanned to form a 1, 1.5 or 1.75° square imaging raster, using a 15 KHz horizontal resonant optical scanner and a 16 Hz vertical optical scanner. Synchronous modulation of the light sources turned them on at the start of the imaging portion of each horizontal line used for imaging when scanning from left to right.

For AOSLO FA imaging, the fluorescence excitation light source used was a 488 nm diode laser (Lasos, Lasertechnick GmbH, Jena, Germany), with an interferometric band-pass optical filter centered at 525 nm and 45 nm bandwidth in front of the detector. This was addressed by using a 3.75x Airy disk diameter confocal pinhole. No attempt was made to compensate for longitudinal chromatic aberration variation among individuals. The reflectance channel light source was a superluminescent laser (SLD) with peak wavelength centered at 790 nm (Superlum Ireland, Carrigtwohill, County Cork, Ireland). The confocal pinhole size was approximately 1x and 16.67x the Airy disk diameter, as measured at the detector plane, for the AOSLO confocal reflectance and OP reflectance imaging, respectively.

2.4 Light safety

The optical powers, without modulation, measured at the cornea, were 15 μW for the 850 nm wavefront sensing superluminescent diode (SLD), 100 μW for the 790 nm imaging SLD and 32 μW for the 488 nm fluorescein excitation diode laser. During imaging, the on/off modulation reduced the average powers delivered to approximately 25% of their original values. All sources were considered as lasers for the maximum permissible exposure (MPE) calculations. Light exposure calculations were determined to be 6

[Citation: Journal/Monograph Title, Vol. XX, No. X (yyyy): pg. XX-XX. DOI. This article is © [Publisher's Name] and permission has been granted for this version to appear in e-Publications@Marquette. [Publisher] does not grant permission for this article to be further copied/distributed or hosted elsewhere without the express permission from [Publisher].]

***NOT THE PUBLISHED VERSION;* this is the author's final, peer-reviewed manuscript.** The published version may be accessed by following the link in the citation at the bottom of the page.

times below MPE according to the American National Standards Institute ANSI Z136 [30].

2.5 Subject alignment and fixation

Each subject was stabilized using a dental impression on a bite bar (Splash! Putty, DenMat Holdings, LLC, Lompoc, California, USA). The bite bar was attached to a three axis translation stage for fine transverse and axial adjustment during imaging.

Subjects were instructed to direct their gaze either towards a green internal fixation target or the corners of the imaging raster. Because of light safety considerations, no retinal location was exposed to the combined light sources (488, 790, and 850 nm) for longer than 120 seconds. Coordinates of these fixation locations were recorded so that the corresponding retinal locations could be imaged accurately and repeatedly. Throughout the imaging session, subjects were encouraged to blink frequently to maintain their normal tear film and were provided with short breaks, at regular intervals or as needed.

2.6 AOSLO FA and AOSLO confocal reflectance imaging

For AOSLO FA, 20 mg/kg oral fluorescein (AK-FLUOR 10%, Akorn, Inc., Lake Forest, Illinois) was administered with orange juice to mask its taste. The use of oral fluorescein has recently been demonstrated to be effective and safe for AOSLO FA imaging in human eyes [18]. Depending on the subject weight, 3-4 vials of fluorescein was administered orally with 50 mL of orange juice to mask its taste. An additional 50 mL of orange juice was provided to wash out any residual taste of the fluorescein. 15 minutes post-administration, simultaneous confocal reflectance and fluorescence image sequences were acquired at each region of interest as previously described [18], consisting of 125 frames at a frame rate of 15 Hz and using a 1.75° field of view (FOV). During AOSLO FA and AOSLO confocal imaging, the retina was simultaneously exposed to three different light sources (488, 790 and 850 nm). The overall imaging time was approximately 15 minutes including short breaks as needed.

[Citation: Journal/Monograph Title, Vol. XX, No. X (yyyy): pg. XX-XX. DOI. This article is © [Publisher's Name] and permission has been granted for this version to appear in e-Publications@Marquette. [Publisher] does not grant permission for this article to be further copied/distributed or hosted elsewhere without the express permission from [Publisher].]

***NOT THE PUBLISHED VERSION;* this is the author's final, peer-reviewed manuscript.** The published version may be accessed by following the link in the citation at the bottom of the page.

2.7 AOSLO OP reflectance imaging

AOSLO OP reflectance imaging of retinal microvasculature has been extensively described in previous reports [14, 16]. Briefly, the technique involves displacement of a larger confocal pinhole, located at the retinal plane conjugate in front of the detector. In this study, retinal microvasculature contrast was maximized by manually displacing the confocal pinhole along the x and/or y axis. Typically, displacing the confocal pinhole orthogonally to the orientation of the retinal vessel being imaged enhanced the visibility of the vascular wall structure and blood flow over a 1 or 1.5° FOV [14, 16]. During AOSLO OP reflectance imaging, the retina was simultaneously exposed to two different light sources (790 and 850nm). The overall imaging time was approximately 30 minutes including short breaks as needed.

2.8 AOSLO image processing

After AOSLO confocal reflectance and AOSLO FA imaging, the fluorescence sequences were co-registered with the confocal reflectance sequences using custom software. Respective images with high signal-to-noise ratio were then generated by averaging the 5-100 frames in each registered sequence [31], resulting in AOSLO confocal structural images and AOSLO FA perfusion maps. For AOSLO OP reflectance imaging, image sequences were registered and averaged, resulting in AOSLO OP structural images. As an additional step, AOSLO OP registered sequences (~100 frames per sequence) were used to create AOSLO OP perfusion maps using the motion contrast technique as described previously [13, 14]. Montages were created using Adobe Photoshop CS6 (Adobe Systems, Inc., San Jose, CA). The flow chart of the image processing for different imaging techniques is illustrated in Fig. 1.

2.9 Comparisons of AOSLO imaging techniques

In order to compare AOSLO FA and OP imaging, three different retinal locations were chosen 1) the foveal capillary network, where the retina was thin (~250 μm), 2) 5° from the foveal center where the retina was relatively thicker (~300 μm), and 3) the peripapillary capillary network where the retina was thickest (~350 μm) and contained multiple capillary plexuses. The foveal avascular zone (FAZ)

[Citation: Journal/Monograph Title, Vol. XX, No. X (yyyy): pg. XX-XX. DOI. This article is © [Publisher's Name] and permission has been granted for this version to appear in e-Publications@Marquette. [Publisher] does not grant permission for this article to be further copied/distributed or hosted elsewhere without the express permission from [Publisher].]

***NOT THE PUBLISHED VERSION;* this is the author's final, peer-reviewed manuscript.** The published version may be accessed by following the link in the citation at the bottom of the page.

was delineated manually on a layer mask of both the AOSLO FA and AOSLO OP perfusion maps in Adobe Photoshop CS6 (Adobe Systems Inc, San Jose, CA). FAZ area in mm^2 and effective diameter (diameter of a theoretical circle with the same FAZ area) were then computed based on these masks using MATLAB (The MathWorks, Inc., Natick, MA)

Additionally, any retinal pathologies evident during the sessions were imaged in order to highlight discrepancies between the two imaging techniques. Five prevalent retinal microangiopathies found in the patients were examined, including 1) microaneurysms; 2) vessel remodeling including vessel looping and collateral formations; 3) leakage; 4) non-perfused blood vessels; and, 5) macular drusen.

3. **Results and discussion**

3.1 General comparison

Although the light levels were maintained well below the ANSI standard during both imaging sessions, the additional short wavelength 488 nm used for AOSLO FA imaging posed a potential increased risk of photochemical damage to the retina [32, 33]. While oral administration of fluorescein has been shown to be safer than IV administration [20, 21], OP reflectance imaging eliminates any need for a contrast agent, further enhancing the safety of the procedure [14].

3.2 Imaging at different retinal regions in healthy subjects

Foveal capillary network

A well-defined FAZ was seen in all three healthy subjects on both AOSLO FA and AOSLO OP perfusion maps (Fig. 2). The mean (± SD) of FAZ area measured on the AOSLO FA and AOSLO OP perfusion maps was 0.297 mm^2 (± 0.06) and 0.301 mm^2 (± 0.06) respectively, resulting in a 1.3% difference in the mean FAZ area and 0.8%

[Citation: Journal/Monograph Title, Vol. XX, No. X (yyyy): pg. XX-XX. DOI. This article is © [Publisher's Name] and permission has been granted for this version to appear in e-Publications@Marquette. [Publisher] does not grant permission for this article to be further copied/distributed or hosted elsewhere without the express permission from [Publisher].]

***NOT THE PUBLISHED VERSION;* this is the author's final, peer-reviewed manuscript.** The published version may be accessed by following the link in the citation at the bottom of the page.

difference in mean FAZ effective diameter between the two imaging approaches. All FAZ area measurements were performed on the original perfusion maps. These FAZ areas are in close agreement with previous studies using conventional FA [34, 35] and AOSLO confocal motion contrast [10, 13] in healthy subjects. Figure 2 (right column) shows the superimposed AOSLO FA (green) and OP perfusion maps (red) after bidirectional elastic image registration using ImageJ plugin bUnwarpJ [36]. All capillaries captured on the AOSLO OP perfusion maps were also identified on the AOSLO FA perfusion maps within a 2.4° diameter (~700 μm) centered at the fovea, and appear to be located in a single layer, in agreement with previous histological studies [37]. These findings suggest that AOSLO OP is an effective noninvasive alternative to FA for assessing the perfused foveal capillary network.

Perifoveal and peripapillary capillary network

Both AOSLO FA and AOSLO OP perfusion maps documented the inner capillary layer showing clear arteriolar capillary free zones (Figs. 3 and 4). In thicker regions of the retina, at a given axial focus, AOSLO FA perfusion map (Figs. 3(A) and 4(B)) is able to capture multiple layers of capillaries at a single time including the inner and outer retinal capillary layers compared to AOSLO OP perfusion map (Figs. 3(C) and 4(E)). This is probably due to the phenomenon that there is no structural background to the AOSLO FA images since only fluorescence is recorded. This in turn enhances the relatively lower contrast of capillaries located above and below the focal imaging plane. Unlike AOSLO FA image, images acquired by AOSLO OP reflectance have a uniform background, reducing the visibility of these capillaries. However, AOSLO OP perfusion map is able to capture multiple capillary networks by adjusting the focus to different depths while imaging and subsequently superimposing these serial images. Also note that the visualization of single file flow of red blood cells within peripapillary capillaries in Fig. 4(E) (Media 1).

Figure 3(B) and 3(D) show the same perifoveal arteriole with a 50 μm lumen diameter captured on AOSLO confocal structural and AOSLO OP structural images, respectively. Vascular wall fine structure including vascular mural cells are readily visualized by AOSLO OP

[Citation: Journal/Monograph Title, Vol. XX, No. X (yyyy): pg. XX-XX. DOI. This article is © [Publisher's Name] and permission has been granted for this version to appear in e-Publications@Marquette. [Publisher] does not grant permission for this article to be further copied/distributed or hosted elsewhere without the express permission from [Publisher].]

***NOT THE PUBLISHED VERSION;* this is the author's final, peer-reviewed manuscript.** The published version may be accessed by following the link in the citation at the bottom of the page.

structural image (Fig. 3(D), black arrow), but not on AOSLO confocal structural image (Fig. 3(B)). The enhanced visibility of the vascular wall fine structure is achieved because the off-centered pinhole simultaneously blocks the direct back scattered light from the overlaying retinal nerve fiber layer and collects multiply scattered light [14, 16].

3.3 Imaging in patients with different retinal pathologies

A variety of retinal vascular abnormalities were studied using AOSLO confocal reflectance, FA, and OP reflectance imaging, including microaneurysms, vascular luminal clot, vessel looping, engorged and dilated blood vessels, vascular leakage, non-perfusion and capillary dropout, tortuous blood vessels, and irregular vessel lumen diameter.

Microaneurysms

Figure 5 shows a microaneurysm in the superior retina 6° above the fovea in a 49 year old female with DR. The AOSLO OP structural images and perfusion maps reveal a relatively normal inner capillary layer (Fig. 5(A) and 5(C)), while a 30 μm diameter microaneurysm can be seen by shifting the focus 120 μm deeper towards the outer retina (Fig. 5(B) and 5(D)). This is consistent with histological studies that localize most diabetic microaneurysms to the outer capillary plexus within the inner nuclear layer [38, 39]. Images with depth information can be created by superimposing serial AOSLO OP perfusion maps as illustrated in Fig. 5(F).

In AOSLO FA, fluorescein dye in the blood stream outlines the perfused retinal vasculature. AOSLO OP motion contrast image processing, on the other hand, employs motion of erythrocytes and/or leukocytes as the intrinsic marker of perfusion. Pixel intensity in the AOSLO FA perfusion map represents fluorescein dye accumulation, whereas the pixel intensity on the AOSLO OP perfusion map represents the blood flow. While the two perfusion maps appear similar, care must be exercised during interpretation or when comparisons are attempted for diagnostic or investigative purposes. An example

[Citation: Journal/Monograph Title, Vol. XX, No. X (yyyy): pg. XX-XX. DOI. This article is © [Publisher's Name] and permission has been granted for this version to appear in e-Publications@Marquette. [Publisher] does not grant permission for this article to be further copied/distributed or hosted elsewhere without the express permission from [Publisher].]

***NOT THE PUBLISHED VERSION;* this is the author's final, peer-reviewed manuscript.** The published version may be accessed by following the link in the citation at the bottom of the page.

demonstrating these differences is shown in Fig. 6, in which various blood pooling and flow patterns of retinal microaneurysms were captured in the temporal retina in a 47 year old male with hypertensive retinopathy. Pooling of the blood is indicated by a relatively higher pixel intensity inside the microaneurysms than in the surrounding capillaries in the AOSLO FA perfusion map (Fig. 6(A), Media 2 and Media 3). A more complex structure of these microaneurysms is revealed by the AOSLO confocal structural and OP structural images, including vessel wall features and luminal clotting with infiltration, as demonstrated in Fig. 6(B) and 6(D). Unlike AOSLO FA, AOSLO OP perfusion maps (Fig. 6(C)) show relatively lower pixel intensity on the lower part of the microaneurysm than the upper part (Fig. 6(A) and 6(C), white arrows). This suggests that while a greater concentration of fluorescein dye was present in the lower part of this microaneurysm, the blood flow velocity was relatively slower when compared to the upper part. The registered AOSLO OP structural videos of the two corresponding microaneurysms (Fig. 6(D)) demonstrate a range of blood flow velocities (Media 4 and Media 5) and confirm the intensity discrepancy between AOSLO FA and AOSLO OP perfusion maps. It is anticipated that with the addition of a higher frame rate, AOSLO OP may provide a unique opportunity to study the flow dynamics of microaneurysms with different morphologies.

Vessel remodeling

Vascular remodeling at various stages including vessel looping, capillary dropout and engorged/tortuous blood vessels were seen in all patients with vasculopathies. Figure 7 demonstrates these phenomena in a 55 year old female with BRVO. Both AOSLO confocal and OP structural images showed vessel looping of an arteriole (Fig. 7(A) and 7(C)). The corresponding AOSLO FA and OP perfusion maps revealed a capillary dropout region (Fig. 7(B) and 7(D), white arrows) and vessel looping (Fig. 7(B) and 7(D), white arrow heads). Figures 7(E) and 7(F) show a magnified structural image of the regions enclosed in the white boxes in Figs. 7(A) and 7(C). While the fine structure of blood vessel wall (Fig. 7(F), black arrows) could be readily distinguished on the AOSLO OP structural image, only limited vessel wall detail could be extracted from the AOSLO confocal structural image. Figure 7(G) shows a magnified AOSLO OP structural image of the region enclosed

[Citation: Journal/Monograph Title, Vol. XX, No. X (yyyy): pg. XX-XX. DOI. This article is © [Publisher's Name] and permission has been granted for this version to appear in e-Publications@Marquette. [Publisher] does not grant permission for this article to be further copied/distributed or hosted elsewhere without the express permission from [Publisher].]

***NOT THE PUBLISHED VERSION;* this is the author's final, peer-reviewed manuscript.** The published version may be accessed by following the link in the citation at the bottom of the page.

in the black box in Fig. 7(C), showing an uneven lumen diameter of the arteriole (large black arrow), vessel looping (white arrow), and non-perfused capillaries (small black arrows).

Leakage and non-perfused blood vessels

Blood vessel leakage could only be detected on AOSLO FA perfusion maps. Figure 8 shows a foveal capillary network (~1.5° superior temporal) in a 62 year old female with CRVO. The AOSLO FA perfusion map shows focal leakage, indicated by the white arrow in Fig. 8(B). In contrast, AOSLO confocal and AOSLO OP structural images and AOSLO OP perfusion maps do not have the capability to show leakage (Fig. 8(A), 8(C), and 8(D)). Fluorescein leakage has been shown to be useful in assessing inner blood-retinal barrier function and retinal vascular endothelial integrity [40, 41], as well as for monitoring response to treatment. AOSLO OP structural images, however, were able to reveal non-perfused blood vessels (Fig. 8(C), black arrows), which were clearly absent on both AOSLO FA and OP perfusion maps. Furthermore, AOSLO FA perfusion maps may be more sensitive to detecting blood vessels with slower or weaker perfusion than AOSLO OP perfusion maps. Figure 8(B) (yellow arrow head) shows a weakly perfused capillary with lower FA signal intensity. The same capillary appears as non-perfused on the AOSLO OP perfusion map (Fig. 8(D), yellow arrow head), possibly due to a slower flow of blood cells.

Perfusion map artifacts

Both the AOSLO FA imaging and AOSLO OP motion contrast processing techniques are subject to artifacts that may appear as vascular flow. AOSLO FA perfusion maps occasionally contain fluorescent structures which do not represent fluorescein movement. AOSLO OP perfusion maps may also show motion artifacts that does not appear to originate from blood cell motion.

Figure 9 shows a comparison of the AOSLO FA and OP perfusion maps at ~1° superior temporal to the fovea in a 37 year old female with macular drusen. While an intact foveal capillary network is clearly

[Citation: Journal/Monograph Title, Vol. XX, No. X (yyyy): pg. XX-XX. DOI. This article is © [Publisher's Name] and permission has been granted for this version to appear in e-Publications@Marquette. [Publisher] does not grant permission for this article to be further copied/distributed or hosted elsewhere without the express permission from [Publisher].]

***NOT THE PUBLISHED VERSION;* this is the author's final, peer-reviewed manuscript.** The published version may be accessed by following the link in the citation at the bottom of the page.

visualized in the AOSLO confocal structural image (Fig. 9(A)), the corresponding AOSLO FA perfusion map shows two diffuse hyperfluorescent regions appearing to emanate from the capillaries like microaneurysms (Fig. 9(B), white arrows). Since these structures do not appear on the AOSLO confocal structural images, the probable source of this hyperfluorescence is macular drusen and the autofluorescent property of RPE lipofuscin [42]. Two corresponding hyper-reflective regions were captured on the AOSLO OP structural image (Fig. 9(C), black arrows). Compared to the AOSLO confocal structural image, the enhanced visualization of macular drusen on the AOSLO OP structural image suggests that the majority of the light returning from the drusen is multiply scattered light [43, 44]. This implies that some retinal features can be imaged better using an AOSLO tuned intentionally for collecting multiply scattered light instead of direct back scattered light. This also suggests a potential application of AOSLO OP reflectance imaging for studying age-related macular degeneration. The AOSLO OP perfusion map of the same region also shows an intact capillary network (Fig. 9(D)).

Clear motion artifacts, or a non-vascular origin, observed in some AOSLO OP perfusion maps (Fig. 3(C), black arrow & Fig. 7(D)) can be recognized by comparison with AOSLO FA perfusion maps. Artifacts in the AOSLO OP perfusion maps along the vessel wall suggest an imperfection of image registration causing non-blood flow related intensity variations. Further improvements to the AOSLO OP image registration technique may help eliminate these spurious motion artifacts. Table 1 summarizes the capabilities of the different techniques for retinal microvasculature imaging.

4. Conclusions

We have demonstrated that AOSLO OP provides retinal microvascular images comparable to those obtained with AOSLO FA with additional structural information such as vessel wall details. The non-invasive nature of AOSLO OP imaging makes it a very appealing imaging tool for screening and monitoring vasculopathies in the retina. AOSLO FA, however, uniquely demonstrates breakdown of the blood-retinal barrier sufficient to allow leakage and may be more sensitive for revealing marginally perfused capillaries with slower blood flow. The complementary information, these techniques provide, enhances

[Citation: Journal/Monograph Title, Vol. XX, No. X (yyyy): pg. XX-XX. DOI. This article is © [Publisher's Name] and permission has been granted for this version to appear in e-Publications@Marquette. [Publisher] does not grant permission for this article to be further copied/distributed or hosted elsewhere without the express permission from [Publisher].]

***NOT THE PUBLISHED VERSION;* this is the author's final, peer-reviewed manuscript.** The published version may be accessed by following the link in the citation at the bottom of the page.

our appreciation of the complexity of the retinal microvascular networks more than could be achieved using either technique alone. Moreover, both techniques offer the ability of detecting subclinical microvascular changes which will become increasingly valuable as we move towards earlier therapeutic management of these diseases.

Acknowledgments

Funding was provided by Marrus Family Foundation, Bendheim-Lowenstein Family Foundation, Wise Family Foundation, Chairman's Research Fund of the New York Eye, Glaucoma Research Foundation Catalyst for a Cure initiative and Ear Infirmary, an unrestricted departmental grant from Research to Prevent Blindness and the GlaucomaResearch Foundation. NIH grants P30EY001931, UL1RR031973 and T32GM07356. Alfredo Dubra-Suarez is the recipient of a Career Development Award from Research to Prevent Blindness and a Career Award at the Scientific Interface from the Burroughs Wellcome Fund. This research was also supported by grants from the RD & Linda Peters Foundation and an unrestricted departmental grant from Research to Prevent Blindness. The authors would also like to thank Eric Cheang, Chun Lin Liu, Mathew Birnbaum, Lenny Rostomian, Ahmad Rehmani, Moataz Razeen, and Drew Scoles for their assistance with image processing.

References and links

1. J. A. Kylstra, J. C. Brown, G. J. Jaffe, T. A. Cox, R. Gallemore, C. M. Greven, J. G. Hall, and D. E. Eifrig, "The importance of fluorescein angiography in planning laser treatment of diabetic macular edema," Ophthalmology **106**(11), 2068–2073 (1999).

2. L. A. Yannuzzi, K. T. Rohrer, L. J. Tindel, R. S. Sobel, M. A. Costanza, W. Shields, and E. Zang, "Fluorescein angiography complication survey," Ophthalmology **93**(5), 611–617 (1986).

3. F. J. Ascaso, M. T. Tiestos, J. Navales, F. Iturbe, A. Palomar, and J. I. Ayala, "Fatal acute myocardial infarction after intravenous fluorescein angiography," Retina **13**(3), 238–239 (1993).

[Citation: Journal/Monograph Title, Vol. XX, No. X (yyyy): pg. XX-XX. DOI. This article is © [Publisher's Name] and permission has been granted for this version to appear in e-Publications@Marquette. [Publisher] does not grant permission for this article to be further copied/distributed or hosted elsewhere without the express permission from [Publisher].]

***NOT THE PUBLISHED VERSION;* this is the author's final, peer-reviewed manuscript.** The published version may be accessed by following the link in the citation at the bottom of the page.

4. V. Fineschi, G. Monasterolo, R. Rosi, and E. Turillazzi, "Fatal anaphylactic shock during a fluorescein angiography," Forensic Sci. Int. **100**(1-2), 137–142 (1999).

5. A. S. L. Kwan, C. Barry, I. L. McAllister, and I. Constable, "Fluorescein angiography and adverse drug reactions revisited: the Lions Eye experience," Clin. Experiment. Ophthalmol. **34**(1), 33–38 (2006).

6. D. C. Kalogeromitros, M. P. Makris, X. S. Aggelides, A. I. Mellios, F. C. Giannoula, K. A. Sideri, A. A. Rouvas, and P. G. Theodossiadis, "Allergy skin testing in predicting adverse reactions to fluorescein: a prospective clinical study," Acta Ophthalmol. (Copenh.) **89**(5), 480–483 (2011).

7. K. R. Mendis, C. Balaratnasingam, P. Yu, C. J. Barry, I. L. McAllister, S. J. Cringle, and D. Y. Yu, "Correlation of histologic and clinical images to determine the diagnostic value of fluorescein angiography for studying retinal capillary detail," Invest. Ophthalmol. Vis. Sci. **51**(11), 5864–5869 (2010).

8. D. C. Gray, W. Merigan, J. I. Wolfing, B. P. Gee, J. Porter, A. Dubra, T. H. Twietmeyer, K. Ahamd, R. Tumbar, F. Reinholz, and D. R. Williams, "In vivo fluorescence imaging of primate retinal ganglion cells and retinal pigment epithelial cells," Opt. Express **14**(16), 7144–7158 (2006).

9. D. Scoles, D. C. Gray, J. J. Hunter, R. Wolfe, B. P. Gee, Y. Geng, B. D. Masella, R. T. Libby, S. Russell, D. R. Williams, and W. H. Merigan, "In-vivo imaging of retinal nerve fiber layer vasculature: imaging histology comparison," BMC Ophthalmol. **9**(1), 9 (2009).

10. J. Tam, J. A. Martin, and A. Roorda, "Noninvasive visualization and analysis of parafoveal capillaries in humans," Invest. Ophthalmol. Vis. Sci. **51**(3), 1691–1698 (2010).

11. J. Tam, K. P. Dhamdhere, P. Tiruveedhula, S. Manzanera, S. Barez, M. A. Bearse, Jr., A. J. Adams, and A. Roorda, "Disruption of the retinal parafoveal capillary network in type 2 diabetes before the onset of diabetic retinopathy," Invest. Ophthalmol. Vis. Sci. **52**(12), 9257–9266 (2011).

12. P. Bedggood and A. Metha, "Direct visualization and characterization of erythrocyte flow in human retinal capillaries," Biomed. Opt. Express **3**(12), 3264–3277 (2012).

[Citation: Journal/Monograph Title, Vol. XX, No. X (yyyy): pg. XX-XX. DOI. This article is © [Publisher's Name] and permission has been granted for this version to appear in e-Publications@Marquette. [Publisher] does not grant permission for this article to be further copied/distributed or hosted elsewhere without the express permission from [Publisher].]

***NOT THE PUBLISHED VERSION;* this is the author's final, peer-reviewed manuscript.** The published version may be accessed by following the link in the citation at the bottom of the page.

13. T. Y. Chui, Z. Zhong, H. Song, and S. A. Burns, "Foveal avascular zone and its relationship to foveal pit shape," Optom. Vis. Sci. **89**(5), 602–610 (2012).

14. T. Y. Chui, D. A. Vannasdale, and S. A. Burns, "The use of forward scatter to improve retinal vascular imaging with an adaptive optics scanning laser ophthalmoscope," Biomed. Opt. Express **3**(10), 2537–2549 (2012).

15. J. Tam, K. P. Dhamdhere, P. Tiruveedhula, B. J. Lujan, R. N. Johnson, M. A. Bearse, Jr., A. J. Adams, and A. Roorda, "Subclinical capillary changes in non-proliferative diabetic retinopathy," Optom. Vis. Sci. **89**(5), E692–E703 (2012).

16. T. Y. Chui, T. J. Gast, and S. A. Burns, "Imaging of vascular wall fine structure in the human retina using adaptive optics scanning laser ophthalmoscopy," Invest. Ophthalmol. Vis. Sci. **54**(10), 7115–7124 (2013).

17. M. Lombardo, M. Parravano, S. Serrao, P. Ducoli, M. Stirpe, and G. Lombardo, "Analysis of Retinal Capillaries in Patients with Type 1 Diabetes and Nonproliferative Diabetic Retinopathy Using Adaptive Optics Imaging," Retina **33**(8), 1630–1639 (2013).

18. A. Pinhas, M. Dubow, N. Shah, T. Y. Chui, D. Scoles, Y. N. Sulai, R. Weitz, J. B. Walsh, J. Carroll, A. Dubra, and R. B. Rosen, "In vivo imaging of human retinal microvasculature using adaptive optics scanning light ophthalmoscope fluorescein angiography," Biomed. Opt. Express **4**(8), 1305–1317 (2013).

19. M. Dubow, A. Pinhas, N. Shah, R. F. Cooper, A. Gan, R. C. Gentile, V. L. Hendrix, Y. N. Sulai, J. Carroll, T. Y. Chui, J. Walsh, R. Weitz, A. Dubra, and R. B. Rosen, "Classification of Human Retinal Microaneurysms using Adaptive Optics Scanning Light Ophthalmoscope Fluorescein Angiography," Invest. Ophthalmol. Vis. Sci. In Press (2014).

20. A. P. Watson and E. S. Rosen, "Oral fluorescein angiography: reassessment of its relative safety and evaluation of optimum conditions with use of capsules," Br. J. Ophthalmol. **74**(8), 458–461 (1990).

[Citation: Journal/Monograph Title, Vol. XX, No. X (yyyy): pg. XX-XX. DOI. This article is © [Publisher's Name] and permission has been granted for this version to appear in e-Publications@Marquette. [Publisher] does not grant permission for this article to be further copied/distributed or hosted elsewhere without the express permission from [Publisher].]

***NOT THE PUBLISHED VERSION;* this is the author's final, peer-reviewed manuscript.** The published version may be accessed by following the link in the citation at the bottom of the page.

21. T. Hara, M. Inami, and T. Hara, "Efficacy and safety of fluorescein angiography with orally administered sodium fluorescein," Am. J. Ophthalmol. **126**(4), 560–564 (1998).

22. D. Y. Kim, J. Fingler, J. S. Werner, D. M. Schwartz, S. E. Fraser, and R. J. Zawadzki, "In vivo volumetric imaging of human retinal circulation with phase-variance optical coherence tomography," Biomed. Opt. Express **2**(6), 1504–1513 (2011).

23. S. Zotter, M. Pircher, T. Torzicky, M. Bonesi, E. Götzinger, R. A. Leitgeb, and C. K. Hitzenberger, "Visualization of microvasculature by dual-beam phase-resolved Doppler optical coherence tomography," Opt. Express **19**(2), 1217–1227 (2011).

24. L. An and R. K. Wang, "In vivo volumetric imaging of vascular perfusion within human retina and choroids with optical micro-angiography," Opt. Express **16**(15), 11438–11452 (2008).

25. C. E. Riva, J. E. Grunwald, S. H. Sinclair, and B. L. Petrig, "Blood velocity and volumetric flow rate in human retinal vessels," Invest. Ophthalmol. Vis. Sci. **26**(8), 1124–1132 (1985).

26. S. Wolf, O. Arend, H. Toonen, B. Bertram, F. Jung, and M. Reim, "Retinal capillary blood flow measurement with a scanning laser ophthalmoscope. Preliminary results," Ophthalmology **98**(6), 996–1000 (1991).

27. S. Yazdanfar, A. M. Rollins, and J. A. Izatt, "Imaging and velocimetry of the human retinal circulation with color Doppler optical coherence tomography," Opt. Lett. **25**(19), 1448–1450 (2000).

28. G. Smith and D. A. Atchison, *The eye and visual optical instruments,* 1st ed. (Cambridge University Press, 1997), Vol. Cambridge.

29. A. Dubra and Y. Sulai, "Reflective afocal broadband adaptive optics scanning ophthalmoscope," Biomed. Opt. Express **2**(6), 1757–1768 (2011).

30. "American National Standard Institute, American National Standard for the Safe Use of lasers, ANSI Z136.1-2007 (ANSI, New York, 2007)."

31. D. C. Gray, W. Merigan, J. I. Wolfing, B. P. Gee, J. Porter, A. Dubra, T. H. Twietmeyer, K. Ahamd, R. Tumbar, F. Reinholz, and D. R. Williams, "In

[Citation: Journal/Monograph Title, Vol. XX, No. X (yyyy): pg. XX-XX. DOI. This article is © [Publisher's Name] and permission has been granted for this version to appear in e-Publications@Marquette. [Publisher] does not grant permission for this article to be further copied/distributed or hosted elsewhere without the express permission from [Publisher].]

***NOT THE PUBLISHED VERSION;* this is the author's final, peer-reviewed manuscript.** The published version may be accessed by following the link in the citation at the bottom of the page.

vivo fluorescence imaging of primate retinal ganglion cells and retinal pigment epithelial cells," Opt. Express **14**(16), 7144–7158 (2006).

32. J. I. Morgan, J. J. Hunter, B. Masella, R. Wolfe, D. C. Gray, W. H. Merigan, F. C. Delori, and D. R. Williams, "Light-induced retinal changes observed with high-resolution autofluorescence imaging of the retinal pigment epithelium," Invest. Ophthalmol. Vis. Sci. **49**(8), 3715–3729 (2008).

33. J. J. Hunter, J. I. Morgan, W. H. Merigan, D. H. Sliney, J. R. Sparrow, and D. R. Williams, "The susceptibility of the retina to photochemical damage from visible light," Prog. Retin. Eye Res. **31**(1), 28–42 (2012).

34. A. C. Bird and R. A. Weale, "On the retinal vasculature of the human fovea," Exp. Eye Res. **19**(5), 409–417 (1974).

35. G. H. Bresnick, R. Condit, S. Syrjala, M. Palta, A. Groo, and K. Korth, "Abnormalities of the foveal avascular zone in diabetic retinopathy," Arch. Ophthalmol. **102**(9), 1286–1293 (1984).

36. I. Arganda-Carreras, C. Ó. Sánchez Sorzano, R. Marabini, J. M. Carazo, C. Ortiz-de Solorzano, and J. Kybic, "Consistent and elastic registration of histological sections using vector-spline regularization, ser. Lecture Notes in Computer Science," *Computer Vision Approaches to Medical Image Analysis* **4241**, 85–95 (2006).

37. R. S. Weinhaus, J. M. Burke, F. C. Delori, and D. M. Snodderly, "Comparison of fluorescein angiography with microvascular anatomy of macaque retinas," Exp. Eye Res. **61**(1), 1–16 (1995).

38. J. Moore, S. Bagley, G. Ireland, D. McLeod, and M. E. Boulton, "Three dimensional analysis of microaneurysms in the human diabetic retina," J. Anat. **194**(1), 89–100 (1999).

39. A. W. Stitt, T. A. Gardiner, and D. B. Archer, "Histological and ultrastructural investigation of retinal microaneurysm development in diabetic patients," Br. J. Ophthalmol. **79**(4), 362–367 (1995).

40. S. H. Sarks, D. Van Driel, L. Maxwell, and M. Killingsworth, "Softening of drusen and subretinal neovascularization," Trans. Ophthalmol. Soc. U. K. **100**(3), 414–422 (1980).

[Citation: Journal/Monograph Title, Vol. XX, No. X (yyyy): pg. XX-XX. DOI. This article is © [Publisher's Name] and permission has been granted for this version to appear in e-Publications@Marquette. [Publisher] does not grant permission for this article to be further copied/distributed or hosted elsewhere without the express permission from [Publisher].]

***NOT THE PUBLISHED VERSION;* this is the author's final, peer-reviewed manuscript.** The published version may be accessed by following the link in the citation at the bottom of the page.

41. H. Miller, B. Miller, and S. J. Ryan, "Newly-formed subretinal vessels. Fine structure and fluorescein leakage," Invest. Ophthalmol. Vis. Sci. **27**(2), 204–213 (1986).

42. N. M. Bressler, S. B. Bressler, and S. L. Fine, "Age-related macular degeneration," Surv. Ophthalmol. **32**(6), 375–413 (1988).

43. A. E. Elsner, Q. Zhou, F. Beck, P. E. Tornambe, S. A. Burns, J. J. Weiter, and A. W. Dreher, "Detecting AMD with multiply scattered light tomography," Int. Ophthalmol. **23**(4/6), 245–250 (2001).

44. A. E. Elsner, S. A. Burns, J. J. Weiter, and F. C. Delori, "Infrared imaging of sub-retinal structures in the human ocular fundus," Vision Res. **36**(1), 191–205 (1996).

Fig. 1. Flow chart of image processing for different imaging techniques

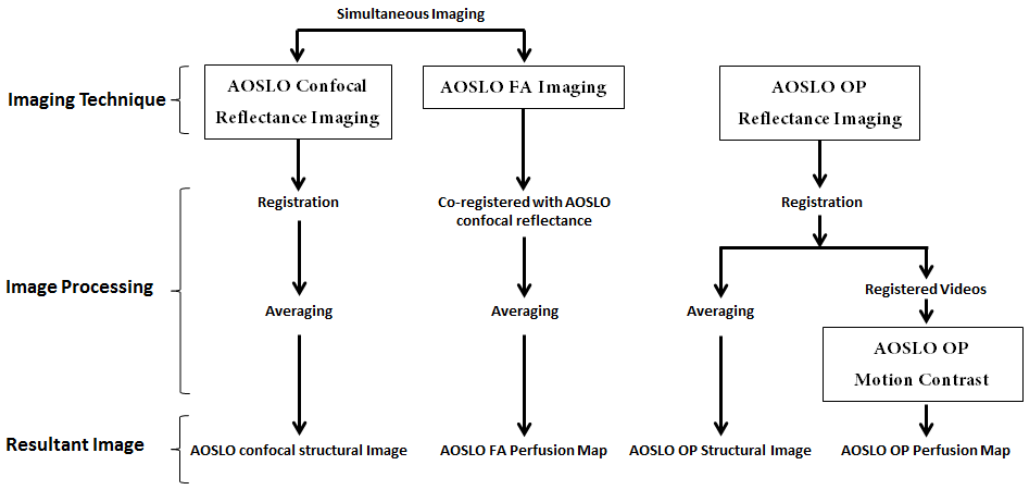

[Citation: Journal/Monograph Title, Vol. XX, No. X (yyyy): pg. XX-XX. DOI. This article is © [Publisher's Name] and permission has been granted for this version to appear in e-Publications@Marquette. [Publisher] does not grant permission for this article to be further copied/distributed or hosted elsewhere without the express permission from [Publisher].]

***NOT THE PUBLISHED VERSION;* this is the author's final, peer-reviewed manuscript.** The published version may be accessed by following the link in the citation at the bottom of the page.

Fig. 2. Comparison of foveal capillary networks imaged using AOSLO FA (left column) and AOSLO OP perfusion maps (middle column) in 3 healthy subjects, after bidirectional elastic image registration. The right column shows the superimposition of the two perfusion maps (AOSLO FA in green and OP in red). Scale bars are 100 μm across. Images have been contrast stretched for display purposes.

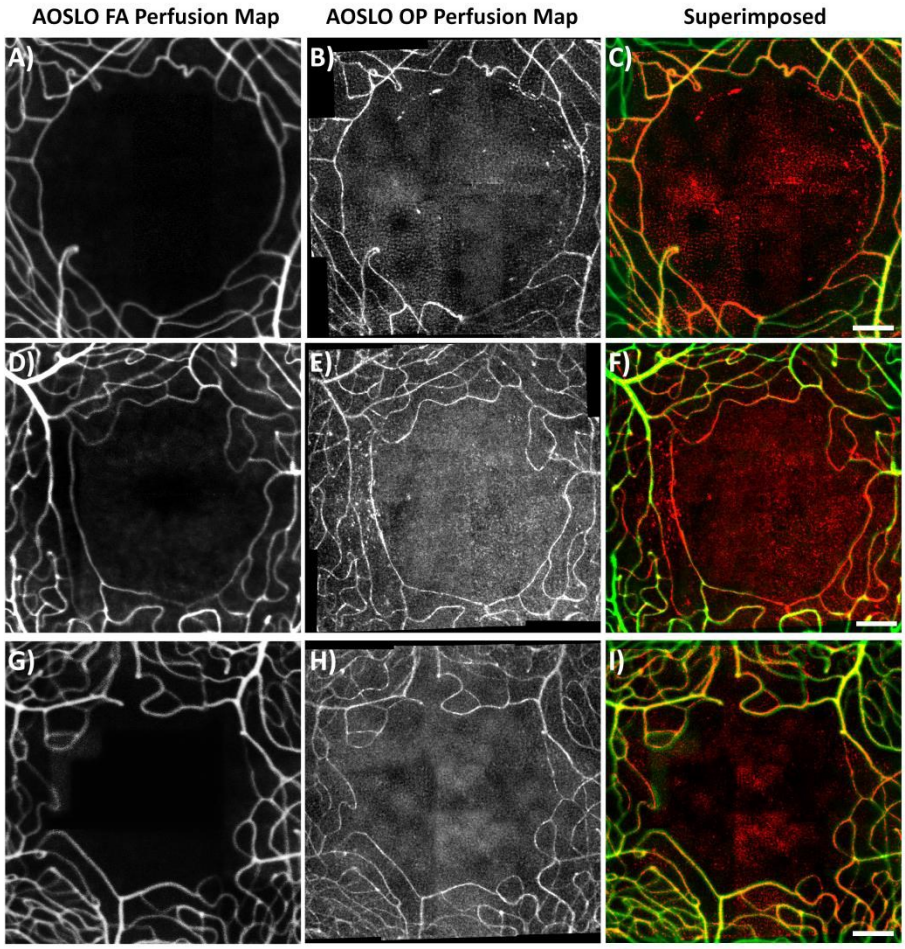

[Citation: Journal/Monograph Title, Vol. XX, No. X (yyyy): pg. XX-XX. DOI. This article is © [Publisher's Name] and permission has been granted for this version to appear in e-Publications@Marquette. [Publisher] does not grant permission for this article to be further copied/distributed or hosted elsewhere without the express permission from [Publisher].]

***NOT THE PUBLISHED VERSION;* this is the author's final, peer-reviewed manuscript.** The published version may be accessed by following the link in the citation at the bottom of the page.

Fig. 3. Comparison of perifoveal (5° above the fovea) microvasculature imaged using AOSLO FA and OP. A) Multiple capillary plexuses including the inner and outer (white arrows) retinal capillary layers are visible on AOSLO FA perfusion map. Image is shown in logarithmic scale for display purposes. B) The corresponding AOSLO confocal structural image as indicated by the white box in A shows limited visibility of the blood vessel wall fine structure. C) AOSLO OP perfusion map shows less capillary layers and reveals an arteriolar capillary free zone at the inner capillary layer. White arrow indicates the motion artifact induced by the vascular wall structure. D) The corresponding AOSLO OP structural image as indicated by the white box in C. Fine details of arteriolar wall fine structure (black arrow) is visible on the AOSLO OP structural image. Images have been contrast stretched for display purposes.

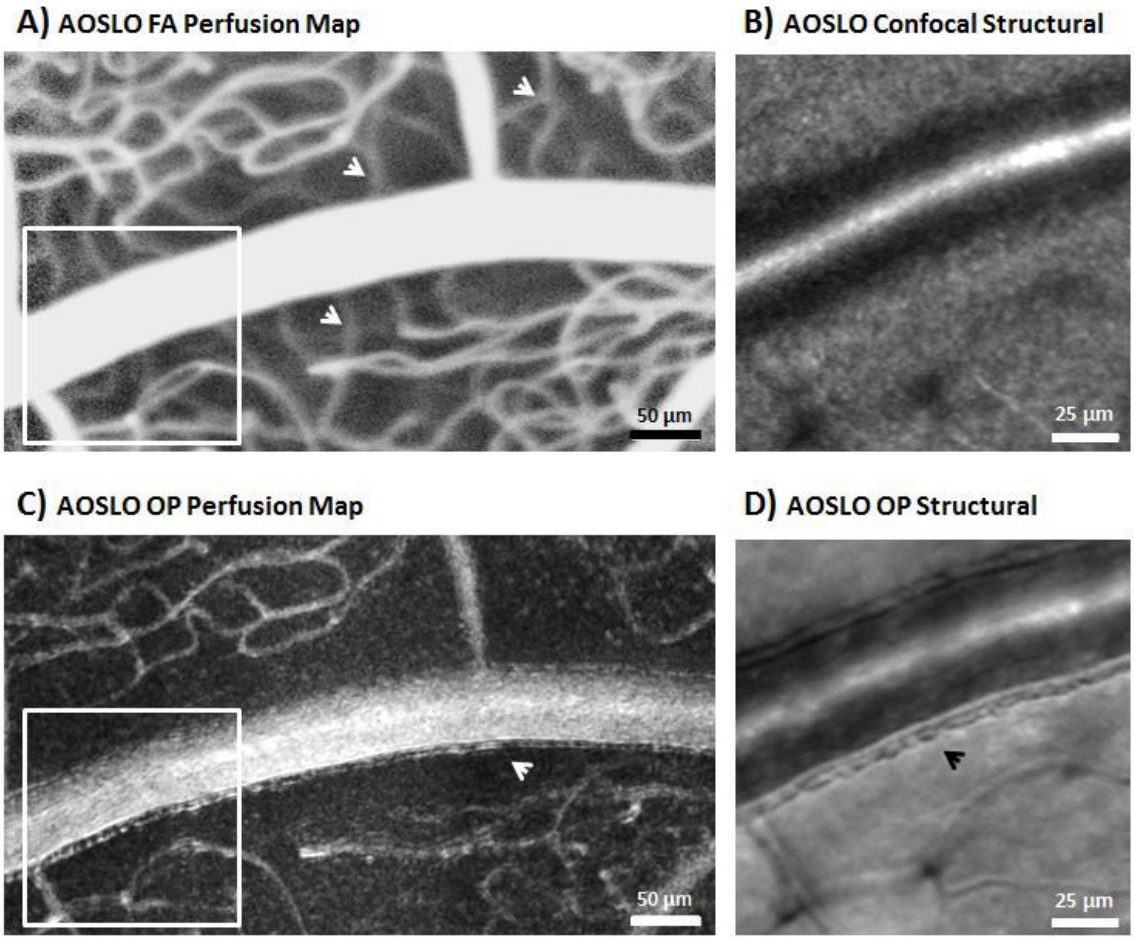

[Citation: Journal/Monograph Title, Vol. XX, No. X (yyyy): pg. XX-XX. DOI. This article is © [Publisher's Name] and permission has been granted for this version to appear in e-Publications@Marquette. [Publisher] does not grant permission for this article to be further copied/distributed or hosted elsewhere without the express permission from [Publisher].]

***NOT THE PUBLISHED VERSION;* this is the author's final, peer-reviewed manuscript.** The published version may be accessed by following the link in the citation at the bottom of the page.

Fig. 4. Comparison of peripapillary microvasculature visualized by AOSLO FA and AOSLO OP perfusion maps. A) Conventional color fundus photograph with regions of interest marked. B-D) AOSLO FA perfusion maps [21] in logarithmic scale for display purposes. E-G) the corresponding AOSLO OP perfusion maps. AOSLO OP structural video (Media 1, scale bar 25 μm) of the black box region in E shows single file flow of red blood cells within capillaries. While both types of perfusion maps are focused at the inner retinal layer, only AOSLO FA show capillaries originating from both the inner and outer retinal layers. Panels B-D were reproduced with permission from the Optical Society. Scale bars are 25 μm. Images have been contrast stretched for display purposes.

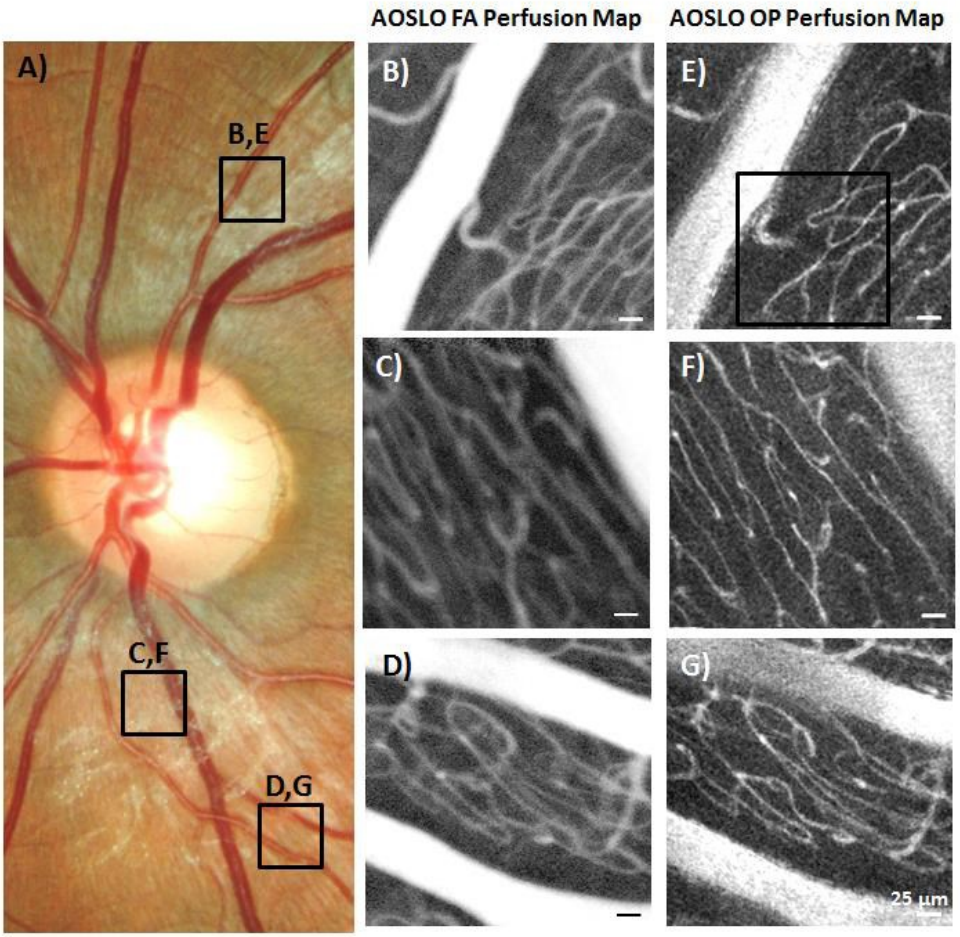

[Citation: Journal/Monograph Title, Vol. XX, No. X (yyyy): pg. XX-XX. DOI. This article is © [Publisher's Name] and permission has been granted for this version to appear in e-Publications@Marquette. [Publisher] does not grant permission for this article to be further copied/distributed or hosted elsewhere without the express permission from [Publisher].]

***NOT THE PUBLISHED VERSION;* this is the author's final, peer-reviewed manuscript.** The published version may be accessed by following the link in the citation at the bottom of the page.

Fig. 5. Comparison of retinal microvasculature located at 6° above the fovea in a 49 year old female with DR. A) The AOSLO OP structural image shows a relatively normal vasculature when focused at the inner retinal layer. B) When focusing at the outer retinal layer, the AOSLO OP structural image reveals a 30 μm microaneurysm at the same retinal location. C & D). The corresponding AOSLO OP perfusion maps of A & B. E) Multiple capillary layers including the inner and outer capillary plexuses are visible in the corresponding AOSLO FA perfusion map at a single focus. F) Superimposed AOSLO OP perfusion maps C & D showing inner capillary plexus in yellow and outer capillary plexus in red. Scale bars are 50 μm. Images have been contrast stretched for display purposes.

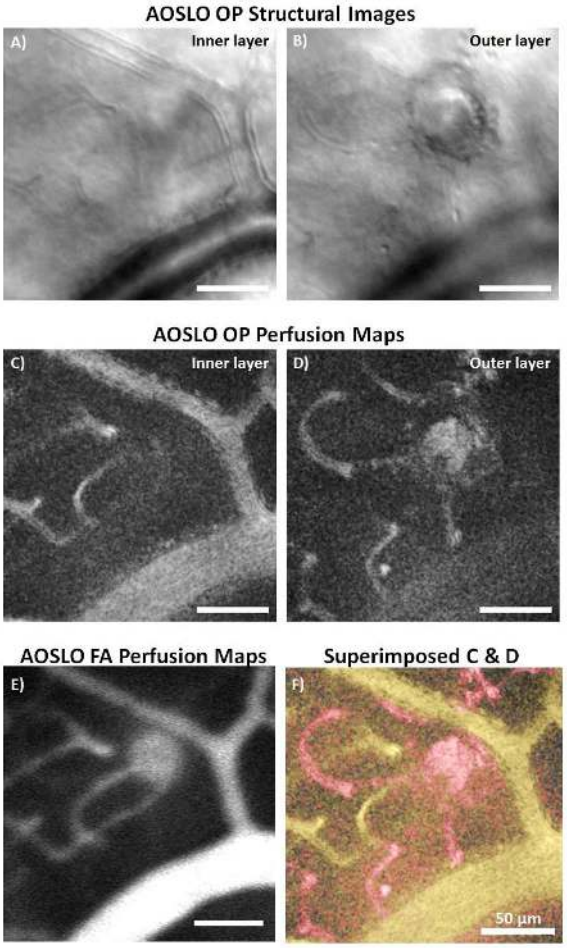

[Citation: Journal/Monograph Title, Vol. XX, No. X (yyyy): pg. XX-XX. DOI. This article is © [Publisher's Name] and permission has been granted for this version to appear in e-Publications@Marquette. [Publisher] does not grant permission for this article to be further copied/distributed or hosted elsewhere without the express permission from [Publisher].]

***NOT THE PUBLISHED VERSION;* this is the author's final, peer-reviewed manuscript.** The published version may be accessed by following the link in the citation at the bottom of the page.

Fig. 6. Comparison of the fluorescein pooling and blood flow pattern of two microaneurysms located at 2° temporal to the fovea in a 47 year old male with HR. A) AOSLO FA perfusion map, showing the pooling of blood content as indicated by the relatively high pixel intensity inside the right microaneurysm (white arrows) (Media 2 and Media 3, scale bars 25 μm). B) The corresponding AOSLO confocal structural image, showing two distinct microaneurysm morphologies. C) AOSLO OP perfusion map showing the same microaneurysms. White arrows indicate the relatively low pixel intensity when compared to A. The black circle in the center of the microaneurysm on the left was due the saturated pixel intensity on the AOSLO OP structural video. D) AOSLO OP structural image. The corresponding structural videos of the microaneurysms demonstrate a range of blood flow velocities (Media 4 and Media 5, scale bars 25 μm). Images have been contrast stretched for display purposes.

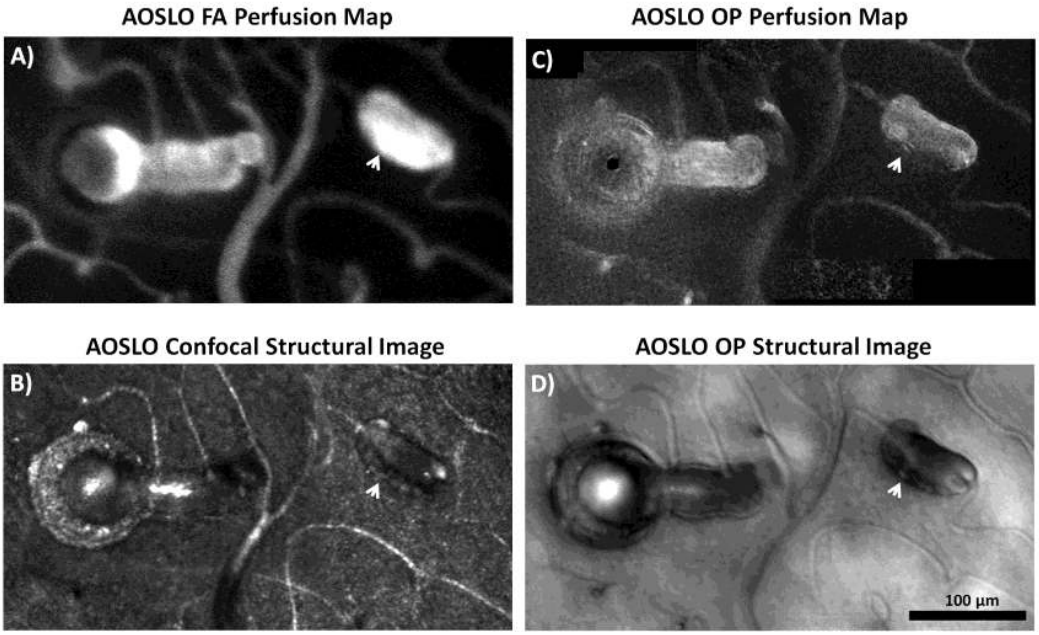

[Citation: Journal/Monograph Title, Vol. XX, No. X (yyyy): pg. XX-XX. DOI. This article is © [Publisher's Name] and permission has been granted for this version to appear in e-Publications@Marquette. [Publisher] does not grant permission for this article to be further copied/distributed or hosted elsewhere without the express permission from [Publisher].]

***NOT THE PUBLISHED VERSION;* this is the author's final, peer-reviewed manuscript.** The published version may be accessed by following the link in the citation at the bottom of the page.

Fig. 7. Comparison of AOSLO FA and OP images on a 55 year old BRVO patient. A) AOSLO confocal structural image showing vessel remodeling of an arteriole located at ~2.5° superior nasal to the fovea. B) The corresponding AOSLO FA perfusion map showing a region with capillary dropout (white arrow) and vessel looping (white arrow head). C) The same retinal region on AOSLO OP structural image. D) The corresponding AOSLO OP perfusion map showing the same region with capillary dropout (white arrow) and vessel looping (white arrow head). E) The magnified region of the white box in A, as an AOSLO confocal structural image, showing limited detail of the vascular wall fine structure. F) The same region on AOSLO OP structural image revealing the vascular wall fine structure (black arrows). G) Magnified region of the black box in C showing vessel looping (white arrow), lumen diameter changes (large black arrow), and non-perfused capillaries (small black arrows). Images have been contrast stretched for display purposes.

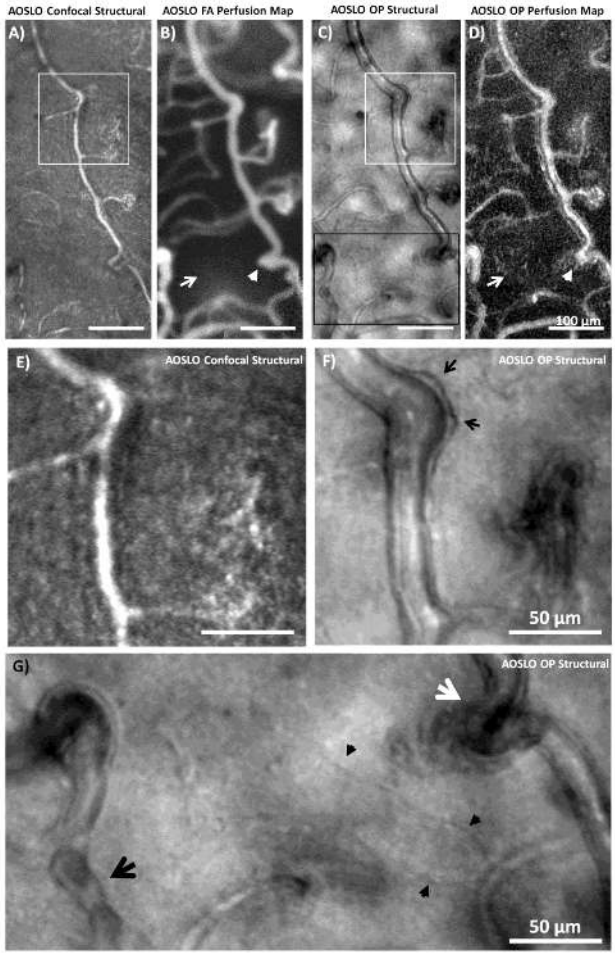

Fig. 8. Comparison of foveal capillary network (~1.5° superior temporal from the fovea) in a 62 year old CRVO patient obtained using

[Citation: Journal/Monograph Title, Vol. XX, No. X (yyyy): pg. XX-XX. DOI. This article is © [Publisher's Name] and permission has been granted for this version to appear in e-Publications@Marquette. [Publisher] does not grant permission for this article to be further copied/distributed or hosted elsewhere without the express permission from [Publisher].]

***NOT THE PUBLISHED VERSION;* this is the author's final, peer-reviewed manuscript.** The published version may be accessed by following the link in the citation at the bottom of the page.

AOSLO FA and OP. A) AOSLO confocal structural image. White arrow head indicates a microaneurysm. B) The corresponding AOSLO FA perfusion map shows focal leakage (white arrow) and a microaneurysm (white arrow head). C) AOSLO OP structural image shows non-perfused blood vessels (black arrows) which are absent from the AOSLO FA and OP perfusion maps. Also shown on the AOSLO OP structural image is the corresponding microaneurysm (white arrow head). D) AOSLO OP perfusion map does not show focal leakage as indicated by the white arrow. White arrow head indicates the corresponding microaneurysm. Yellow arrow heads on A-D indicate a capillary identified as non-perfused on AOSLO OP perfusion map, but shows poor perfusion on the AOLSO FA perfusion map. Images have been contrast stretched for display purposes.

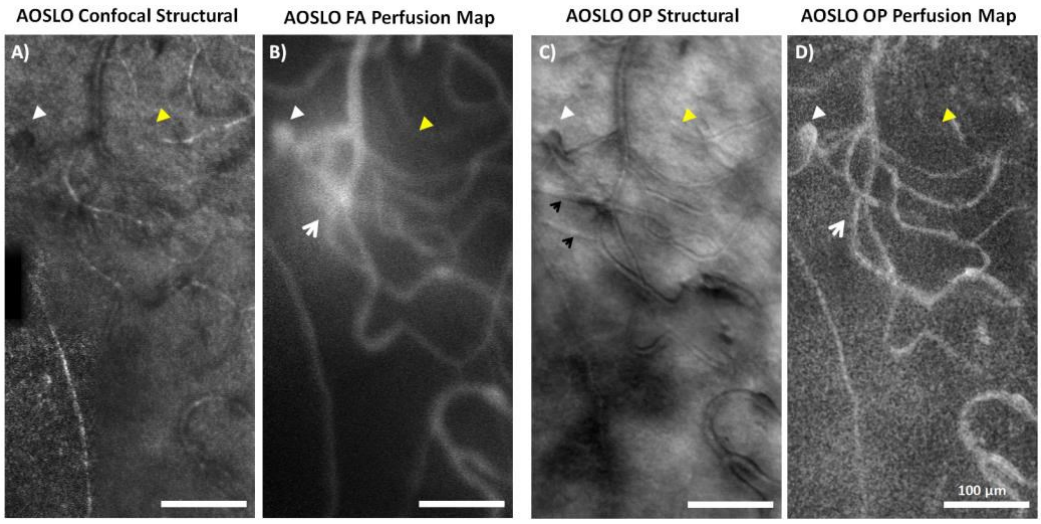

[Citation: Journal/Monograph Title, Vol. XX, No. X (yyyy): pg. XX-XX. DOI. This article is © [Publisher's Name] and permission has been granted for this version to appear in e-Publications@Marquette. [Publisher] does not grant permission for this article to be further copied/distributed or hosted elsewhere without the express permission from [Publisher].]

***NOT THE PUBLISHED VERSION;* this is the author's final, peer-reviewed manuscript.** The published version may be accessed by following the link in the citation at the bottom of the page.

Fig. 9. Comparison of foveal capillary networks (~1° superior temporal from the fovea) in a 37 year old female with macular drusen. A) AOSLO confocal structural image shows an intact capillary network. B) AOSLO FA perfusion map reveals two hyperfluorescent regions mimicking the appearance of microaneurysms, due to underlying drusen autofluorescence (white arrows). C) AOSLO OP structural image shows two diffuse hyper-reflective regions (black arrows) from the same drusen in B. D) AOSLO OP perfusion map shows intact vasculature. Images have been contrast stretched for display purposes.

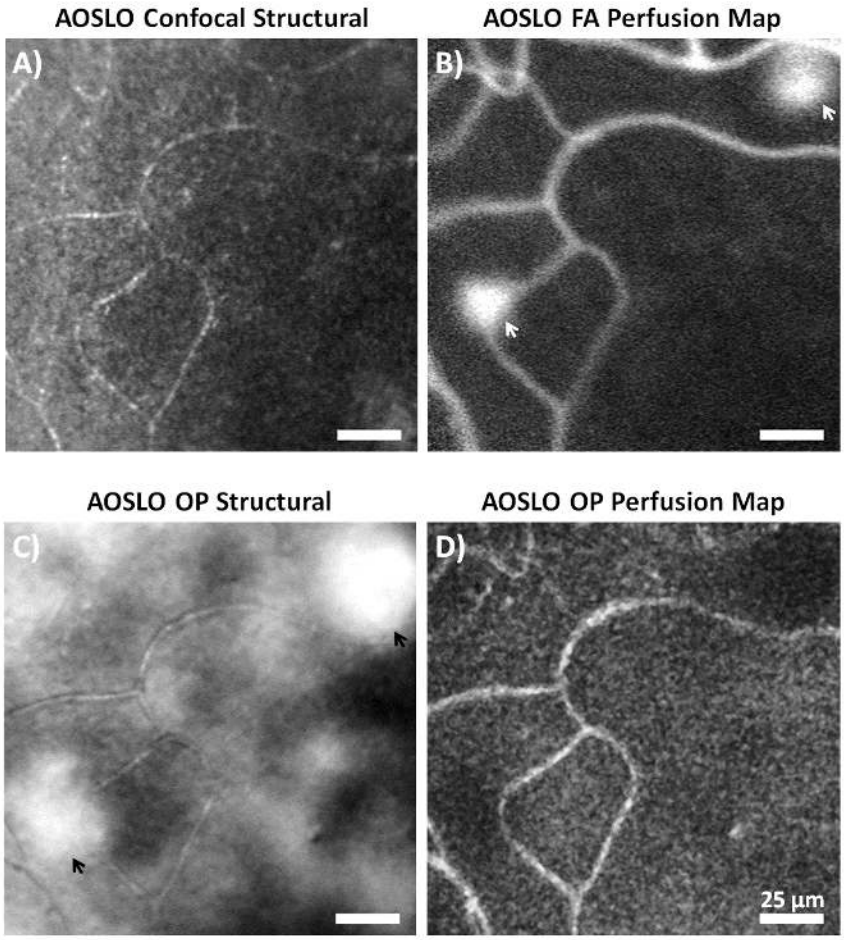

[Citation: Journal/Monograph Title, Vol. XX, No. X (yyyy): pg. XX-XX. DOI. This article is © [Publisher's Name] and permission has been granted for this version to appear in e-Publications@Marquette. [Publisher] does not grant permission for this article to be further copied/distributed or hosted elsewhere without the express permission from [Publisher].]

***NOT THE PUBLISHED VERSION;* this is the author's final, peer-reviewed manuscript.** The published version may be accessed by following the link in the citation at the bottom of the page.

Table 1. Comparison of AOSLO confocal reflectance, FA, OP reflectance, and OP motion contrast techniques

	AOSLO Confocal Reflectance	AOSLO FA	AOSLO OP Reflectance	AOSLO OP Motion Contrast
Imaging Wavelength	790 nm	488 nm	790 nm	NA
Pinhole Size (Airy disk diameter)	1x	3.75x	16.7x	NA
Pinhole Centration	Confocal	Confocal	Offset	NA
Exogenous agent	No	Yes (Oral Fluorescein)	No	No
Resultant Image	AOSLO confocal structural image	AOSLO FA perfusion map (real time)	AOSLO OP structural image	AOSLO OP perfusion map (post processing based on AOSLO OP videos)
Perfusion Map Pixel Intensity	NA	Presence / concentration of fluorescein	NA	Relative blood flow velocity
Capillary Plexuses	Single layer at each focus	multiple layers simultaneously	Single layer at each focus	Single layer at each focus
Vascular Wall Fine Structure Visibility	No	No	Yes	No
Single File Flow of RBCs	No	No	Yes	No
Detect Leakage / Infiltration	No	Yes	No	No
Non Perfused Blood Vessel Visibility	Yes	No	Yes	No
Perfusion Map Artifacts	NA	Autofluorescence	NA	Motion artifact

[1]Department of Ophthalmology, New York Eye & Ear Infirmary, New York, NY 10003, USA

[2]Icahn School of Medicine at Mount Sinai, New York, NY 10029, USA

[3]The Institute of Optics, University of Rochester, Rochester, NY 14627, USA

[4]Department of Biomedical Engineering, Marquette University, Milwaukee, WI 53233, USA

[5]Department of Ophthalmology, Medical College of Wisconsin, Milwaukee, WI 53226, USA

[6]Department of Biophysics, Medical College of Wisconsin, Milwaukee, WI 53226, USA

[7]Department of Ophthalmology, New York Medical College, Valhalla, NY 10595, USA

* rrosen@nyee.edu

[Citation: Journal/Monograph Title, Vol. XX, No. X (yyyy): pg. XX-XX. DOI. This article is © [Publisher's Name] and permission has been granted for this version to appear in e-Publications@Marquette. [Publisher] does not grant permission for this article to be further copied/distributed or hosted elsewhere without the express permission from [Publisher].]